

Acoustic NMR and nonlinear nuclear spin phenomena in hematite

R. A. Bagautdinov, Kh. G. Bogdonova, V. A. Golenishchev-Kutuzov, and G. R. Enikeeva

Kazan' Physicotechnical Institute of the Kazan' Branch of the USSR Academy of Sciences

(Submitted 7 February 1984; resubmitted 6 July 1984)

Zh. Eksp. Teor. Fiz. **87**, 2008–2013 (December 1984)

Acoustic NMR on ^{57}Fe nuclei is observed and investigated. The maximum resonant absorption of ultrasound is 200 cm^{-1} . Some features of the propagation of longitudinal and transverse ultrasound waves in the vicinity of the resonance ($\omega_n/2\pi = 71.2 \text{ MHz}$) are investigated. Restoration of the initial shape of the ultrasound pulses is observed in the vicinity of the NMR at $\omega = \omega_n$ as a result of compensation of the dispersion smearing by the magnetoelastic nonlinearity.

Much attention is being paid¹⁻³ to the study of singularities of magnetoelastic interactions and of the role of spin systems in antiferromagnets with easy magnetization plane (AFEP). Acoustic resonance offers a possibility of expanding this research with an aim of obtaining the dynamic characteristics of magnetic ordering and magnetoelastic interactions. In acoustic NMR, ultrasound waves of NMR frequency induce, via the magnetoelastic (ME) coupling, oscillation of the electron spin system, and excite next the nuclear spin via hyperfine electron-nucleus interaction. When the elastic and nuclear spin branches intersect, strong anharmonicity of the coupled ME system occurs. The use of ultrasound waves with different polarizations, propagation directions, and intensities permits separation of the individual interactions and estimates of their strengths.

Earlier investigations^{4,5} have shown that it is precisely AFEP, which include also hematite, that are characterized by the highest values of the coefficient α_n of resonant spin absorption of ultrasound, which is evidence of the existence of strong spin-phonon interactions. A number of nonlinear acoustic spin phenomena were also observed in the same crystals, such as nuclear spin echo, self-induced transparency, and generation of coherent phonons.^{6,7}

Acoustic NMR was used heretofore to investigate only low-temperature AFEP with strong electron-nucleus interaction that leads to "entanglement" of the electronic and nuclear spin oscillations; this complicated the interpretation of the results. For a high-temperature magnet such as hematite, the influence of the nuclear spin system on the electronic one can be neglected, so that only two coupled systems need be considered, viz., the nuclear spin and elastic systems.

EXPERIMENTAL PROCEDURE

Hematite ($\alpha\text{-Fe}_2\text{O}_3$) with rhombic symmetry of type D_{3d}^6 has, in the interval between the Morin temperature ($T_M \sim 262 \text{ K}$ for an impurity-free crystal) and the Néel temperature ($T_N \sim 948 \text{ K}$), weak ferromagnetism with a magnetization vector oriented in the easy plane (111). The samples investigated were cut from a single ingot, were rectangular parallelepipeds measuring $4 \times 6 \times 1 \text{ mm}$, and had one face oriented, accurate to within one degree, parallel or perpendicular to the [111] axis. Ultrasound pulses in the frequency range 60–80 MHz and of duration 0.5–5 μs were excited and detected by two lithium-niobate piezoelectric elements. Owing to the reflections in the piezoconverters, multiple passes of the ultrasound pulses through the samples were

used. The use of long ($l \sim 16 \text{ mm}$) piezoconverters with surface excitation permits generation of a continuous oscillation spectrum in the indicated range, and separation of each pulse passing through the sample. The phase velocity of the ultrasound pulses propagating through the sample was determined from the spectrum of the size-effect acoustic resonances in the compound sample + piezoconverter resonator. We investigated the changes in the damping and propagation velocity of the ultrasound pulses as functions of the frequency. The damping coefficient α_n is defined as the ratio of the resonantly absorbed energy P_n of an ultrasound wave $u = u_0 \sin(\mathbf{k}\mathbf{r} - \omega t)$ to the flux of the average energy through the sample

$$\alpha_n = P_n / \rho v_{l,t} \varepsilon^2, \quad (1)$$

where ρ is the sample density, $v_{l,t}$ is the longitudinal or transverse propagation velocity, and ε is the amplitude of the ultrasound-wave deformation. At

$$P_n = \frac{1}{2} \omega \chi''(\mathbf{k}, \omega) H_1^2, \quad (a)$$

where

$$\chi''(\mathbf{k}, \omega) = \pi J(J+1) \omega N \gamma_n^2 \hbar^2 g(\omega) / 6kT \quad (b)$$

is the imaginary part of the complex susceptibility of the nuclear spin system, N is the number of magnetic nuclei, γ_n is the nuclear gyromagnetic ratio, $g(\omega)$ is the form factor of the resonances line, we have

$$\alpha_n = \frac{\pi J(J+1) N \gamma_n^2 \hbar^2 H_1^2 g(\omega) \omega^2}{6kT \rho v_{l,t}^3 \varepsilon^2}. \quad (2)$$

The effective magnetic field H_1 acting on the nuclear spins as a result of the ultrasonic deformation can be estimated by using the results of Refs. 4, 11, and 12. Since the dynamic electron-nucleus interaction is effected in hematite only via the low-frequency branch of the spin waves, H_1 can be represented in the following phenomenological form⁴ without allowance for the deviation of the magnetic-anisotropy field \mathbf{H}_A from the \mathbf{H}_0 direction in the (111) plane:

$$H_1 = \frac{H_n H_{ME}}{H_A} \quad \text{at} \quad H_{M^2} = \frac{B_i^2 \varepsilon^2}{M_0^2} \Gamma(\varphi, \theta), \quad (3)$$

where H_n is the projection of the hyperfine field on the nuclear-spin quantization axis, H_{ME} is the magnetoelastic field, M_0 is the modulus of the magnetization vector of one sublattice, B_i are the constants of the dynamic ME coupling, and $\Gamma = \mathbf{k}/|k|$. Thus, at $\omega = \omega_n$ we have

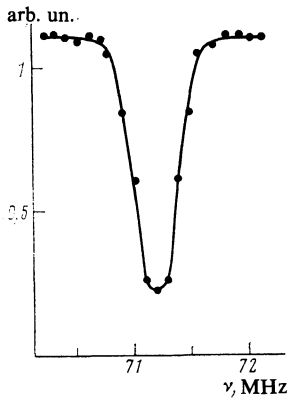


FIG. 1. Line shape of acoustic NMR on ^{57}Fe nuclei in hematite.

$$\alpha_n = \frac{\pi J(J+1)Ng(\omega_n)\omega_n^4 B_i^2 \Gamma(\varphi, \theta) \hbar^2}{6kT\rho v_{i,t}^3 M_0^2 H_A^2} \quad (4)$$

For longitudinal and transverse waves,

$$\Gamma(\varphi, \theta) = \sin^2 \varphi \cdot \sin^2 2\theta, \quad \Gamma(\varphi, \theta) = \frac{1}{4} \sin^2 2\varphi \cdot \sin^2 2\theta,$$

where φ and ϑ are the polar and azimuthal angles of the wave vector \mathbf{k} . Substitution of the values $N = 10^{20} \text{ cm}^{-3}$, $\rho = 5.3 \text{ g}\cdot\text{cm}^{-3}$, $g(\omega_n) = 10^{-4} \text{ s}$, $v_l = 6.8 \cdot 10^5 \text{ cm}\cdot\text{sec}^{-1}$, $v_t = 4.1 \cdot 10^5 \text{ cm}\cdot\text{s}^{-1}$, $H_A = 0.7 \text{ Oe}$, and $M_0 = 870 \text{ Oe}$ (Ref. 2) in expression (4) for different variants of ultrasound propagation yields $B_1 \sim (2.3 \pm 0.7) \cdot 10^{-7} \text{ erg}\cdot\text{cm}^{-3}$ and $B_4 \sim (6 \pm 2) \cdot 10^7 \text{ erg}\cdot\text{cm}^{-3}$, which are close to the values of B_i obtained in the investigation of ME interactions under nonresonant conditions.^{1,2}

The field dependence of α_n can be attributed to participation of the domains in the spin-phonon interaction. As follows from x-ray diffraction investigations,¹³ the 180-degree, of the magnetic-field strength H_0 , and of the temperature in the interval $T_M \leq T \leq 350 \text{ K}$.

RESULTS

Resonant acoustic absorption with center at 71.2 MHz at $T = 293 \text{ K}$ and $H_0 = 0$ (Fig. 1) was observed in the entire investigated temperature interval for propagation of longitudinal-wave pulses with wave vector \mathbf{k}_l along the [111] axis ($\alpha_n 10 \pm 2 \text{ cm}^{-1}$) and with \mathbf{k}_l in the (111) plane ($\alpha_n \sim 60 \pm 6 \text{ cm}^{-1}$), as well as in propagation of transverse-wave pulses

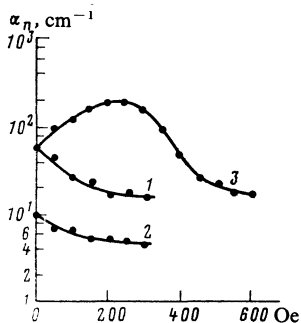


FIG. 2. Field dependence of resonant absorption of ultrasound at $(\mathbf{H}_0 \perp \mathbf{k}_l) \parallel (111)$ (curve 1), $\mathbf{k}_l \parallel [111]$ and $\mathbf{H}_0 \parallel (111)$ (curve 2) and $(\mathbf{H}_0 \parallel \mathbf{k}_l) \parallel (111)$ (curve 3).

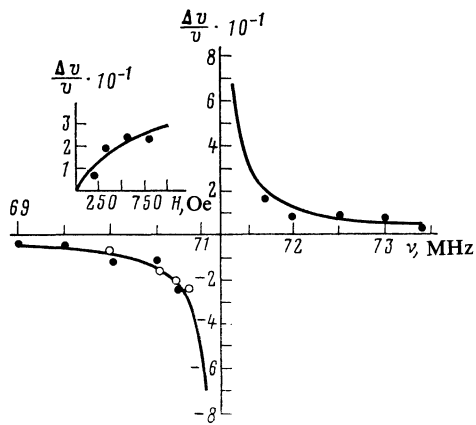


FIG. 3. Frequency and field (inset) dependences of the phase velocity of a longitudinal ultrasound wave: solid lines—theoretical curves; ●—experimental points; ○—experimental points in the case of compensation of the dispersion spreading by the ME interaction.

with vector \mathbf{k}_l and wave polarization ξ , both in the (111) plane ($\alpha_n \sim 45 \pm 15 \text{ cm}^{-1}$). The absorption ceased at $T = T_M = 262 \text{ K}$. With increasing T , the frequency of the resonance decreased practically linearly ($\Delta\nu/\Delta T \sim 15 \text{ kHz/K}$), in agreement with the NMR data for ^{57}Fe in hematite and attributed to the change of the sublattice magnetization.⁸ The absorption line shape was close to Gaussian. These characteristic features of the ultrasound absorption can attribute it to acoustic resonance of the ^{57}Fe nuclei. A dependence of α_n on the magnetic field H_0 applied in the (111) was observed. For a longitudinal wave at $(\mathbf{H}_0 \perp \mathbf{k}_l) \parallel (111)$ the value of α_n decreased smoothly as H_0 was increased to 200 Oe (Fig. 2), after which it remained constant. A similar behavior of α_n was observed also for $\mathbf{k}_l \parallel [111]$ at $\mathbf{H}_0 \parallel (111)$. The hysteresis loop previously observed in a number of NMR investigations at a similar orientation of the vectors of the constant and alternating magnetic fields^{9,10} was not observed in our case. When \mathbf{H}_0 is displaced from the (111) plane, α_n becomes less dependent on H_0 , and at $\mathbf{H}_0 \parallel [111]$ the value of α_n remains constant at $0 < H_0 < 600 \text{ Oe}$. In the case $(\mathbf{H}_0 \parallel \mathbf{k}_l) \parallel (111)$ an increase of α_n to 200 cm^{-1} was observed as H_0 increased to 250 Oe (Fig. 2). This effect was not recorded before in the NMR spectra of ^{57}Fe and in $\alpha\text{-Fe}_2\text{O}_3$.

A change of α_n with increasing H_0 was also observed for transverse waves, but was more complicated. This was caused by propagation of waves with different polarizations, because of the mismatch of the acoustic impedances of the sample and of the piezoconverter.

A change of the phase velocity v_l of the ultrasound pulses passing through the sample was observed near the resonances (Fig. 3). The maximum change of the velocity v_l was $\sim 20\%$ for $\alpha_n = 37 \text{ cm}^{-1}$, with the sign of the dispersion reversed at $\omega = \omega_n$. The propagation of the short ($\tau_p \sim 2 \mu\text{s}$) pulses under strong-dispersion conditions led to distortion of the pulse waveform. The leading and trailing edges of the pulse passing through the sample were distorted at $\omega < \omega_n$ and $\omega > \omega_n$, respectively. At $\omega = \omega_n$ the crest of the pulse was modulated, but the edges were not distorted (Fig. 4). At $\omega < \omega_n$ application of H_0 in the case $(\mathbf{H}_0 \perp \mathbf{k}_l) \parallel (111)$ can compensate for the distortion of the leading edge.

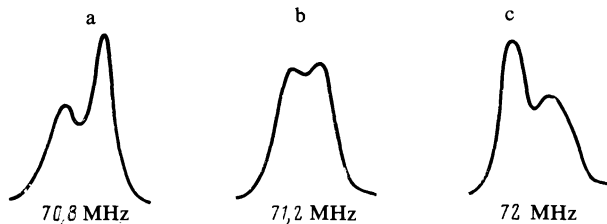


FIG. 4. Dispersion distortion of the pulse waveform: a) $\omega < \omega_n$, b) $\omega = \omega_n$, c) $\omega > \omega_n$.

It must be noted that all our results pertain to samples that have been demagnetized beforehand.

DISCUSSION OF RESULTS

The coefficient α_n of ultrasound absorption by nuclear gree domains in hematite are arranged in layers parallel to the (111) plane, the domains being separated by Néel walls within the layers and by Bloch walls between the layers.

At $H_{0(111)} > H_A$, where $H_{0(111)}$ is the projection of \mathbf{H}_0 on the (111) plane, the antiferromagnetism vector \mathbf{L} is oriented in this plane perpendicular to \mathbf{H}_0 . In the case $(\mathbf{H}_0 \perp \mathbf{k}_l) \parallel (111)$ the vector \mathbf{H}_l is parallel to \mathbf{L} and the direct ME interaction is small. It can be enhanced, however, when the domain walls move under the influence of the ultrasound and produce gradients perpendicular to \mathbf{L} . The sublattice magnetizations in the plane (111) are then appreciably deflected, by an angle $\beta \sim H_{ME}/H_A$, from their initial position in the (111) plane. The vanishing of the domain walls with increasing H_0 , which is confirmed by the field dependence of the spectra of the ordinary NMR,^{9,10} leads to a decrease in the value of α_n .

In the situation $(\mathbf{H}_0 \parallel \mathbf{k}_l) \parallel (111)$ the vector \mathbf{k}_l is perpendicular to \mathbf{L} and the observed additional increase of α_n with increasing H_0 can be attributed to a suppression of the domain walls by the magnetic field, since the energy needed to cause the latter to oscillate comes from the ultrasound wave.

The absorption of ultrasound at $\mathbf{k}_l \parallel [111]$ is also determined by the existence of domain walls, since longitudinal ultrasonic oscillations with $\mathbf{k}_l \parallel [111]$ cannot produce a magnetic field H_l of sufficient strength to move \mathbf{L} out of the (111) plane. In this case H_l is enhanced by ultrasonic modulation of the walls between the domain layers.

As follows from Fig. 1, the acoustic-NMR line ($\Delta\omega/2\pi = 400$ kHz) is greatly broadened compared with the line of the ordinary NMR.⁹ This broadening can be explained by the presence of structure imperfections and defects that lead to inhomogeneity of the anisotropy field H_A .

In view of the strong coupling between the elastic and nuclear spin systems, the absorption α_n is accompanied by dispersion. The corresponding dispersion equation was obtained in Ref. 14. Using its results for $J = 1/2$, we can write the following expression for the change of the phase velocity v_l in the vicinity of the acoustic NMR for $|\omega - \omega_n| > \Delta\omega$:

$$\frac{\Delta v_l}{v_{l0}} = \frac{2\alpha_n T_2^2 v_{l0}}{[1 + (\omega^2 - \omega_n^2) T_2^2] g(\omega_n)}, \quad (5)$$

where T_2 is the time of the nuclear spin-spin relaxation, $\Delta\omega$ is the NMR linewidth, and v_{l0} is the speed of sound in the absence of dispersion. The maximum change of v_l for the points $\omega_n - \Delta\omega$ and $\omega_n + \Delta\omega$ is $\alpha_n v_{l0}^2/\omega$.

The observed change of the phase velocity is well described by expression (5) at $\alpha_n \sim 37$ cm⁻¹ and $T_2 \sim 5 \cdot 10^{-4}$ s (measured by the echo-pulse NMR method). The distortions of the leading or trailing edges of the pulse under conditions of dispersion propagation are attributed to cutoff of the pulse spectrum at the upper and lower frequencies, respectively. At exact resonance the spectrum acquires a central part, and this leads to a uniform phase modulation over the entire length of the rectangular pulse. A similar effect was already observed by us in the vicinity of acoustic NMR of ⁵⁵Mn in KMnF₃ (Ref. 15).

The restoration of the rectangular pulse shape on application of H_0 at $\omega < \omega_n$ can be attributed to compensation of the dispersion spreading of the pulse near ω_n by the nonlinear dispersion of ME interaction of opposite sign; this dispersion is described by the expression¹⁶

$$v_l = \frac{1}{\rho^{1/2}} \left[\frac{1}{2} (c_1 - c_2) - \frac{L^3 (d_1 - d_2)^2}{H_{MY} + H_0 H_D / H_E} \right]^{1/2}, \quad (6)$$

where c_i are the elastic moduli, d_i are the magnetostriction constants, H_D is the Dzyaloshinskii field, and H_E is the exchange field (inset of Fig. 3).

- ¹A. S. Borovik-Romanov and B. G. Rudashevskii, Zh. Eksp. Teor. Fiz. **47**, 2095 (1964) [Sov. Phys. JETP **20**, 1407 (1965)].
- ²V. I. Ozhogin and V. L. Preobrazhenskii, *ibid.* **73**, 988 (1964) [**46**, 523 (1977)].
- ³E. A. Turov, Usp. Fiz. Nauk **140**, 429 (1983) [Sov. Phys. Usp. **26**, 593 (1983)].
- ⁴I. B. Merry and D. I. Bolef, Phys. Rev. **B4**, 1572 (1971).
- ⁵V. R. Gakel', Zh. Eksp. Teor. Fiz. **57**, 1827 (1974) [*sic*].
- ⁶Kh. G. Bogdanova, V. A. Kolenishchev-Kutuzov, A. A. Monakhov, A. V. Kuz'ko, V. P. Lukomskii, and Yu. B. Chovnyuk, Pis'ma Zh. Eksp. Teor. Fiz. **32**, 476 (1980) [JETP Lett. **32**, 360 (1980)].
- ⁷A. M. Smirnov, Zh. Eksp. Teor. Fiz. **84**, 2290 (1983) [Sov. Phys. JETP **57**, 1335 (1983)].
- ⁸G. B. Benedek and J. Armstrong, J. Appl. Phys. **32**, 1065 (1961).
- ⁹A. V. Zalesskii, I. S. Zheludev, and R. A. Voskanyan, Zh. Eksp. Teor. Fiz. **59**, 673 (1970) [Sov. Phys. JETP **32**, 367 (1971)].
- ¹⁰A. Hirai, J. A. Eaton, and C. W. Searle, Phys. Rev. B **3**, 68 (1971).
- ¹¹L. L. Buishvili, Fiz. Tverd. Tela (Leningrad) **5**, 1027 (1963) [Sov. Phys. Solid State **5**, 748 (1963)].
- ¹²S. D. Silverstein, Phys. Rev. **132**, 997 (1963).
- ¹³V. G. Labushkin, A. A. Lomov, N. N. Faleev, and V. A. Figin, Fiz. Tverd. (Leningrad) **22**, 1725 (1980) [Sov. Phys. Solid State **22**, 1006 (1980)].
- ¹⁴E. H. Jacobsen and K. W. H. Stevens, Phys. Rev. **129**, 2036 (1963).
- ¹⁵Kh. G. Bogdanova, R. A. Bagautdinov, V. A. Golenishchev-Kutuzov, and V. P. Lukomskii, Pis'ma Zh. Eksp. Teor. Fiz. **37**, 483 (1983) [JETP Lett. **37**, 574 (1983)].
- ¹⁶V. N. Shcheglov, Fiz. Tverd. Tela (Leningrad) **14**, 2180 (1963) [Sov. Phys. Solid State **14**, 1889 (1964)].

Translated by J. G. Adashko